Article

Mixing Performance of a Suspended Stirrer for Homogenizing Biodegradable Food Waste from Eatery Centers

Olumide Babarinsa [1], Emmanuel O.B. Ogedengbe [1,*] and Marc A. Rosen [2]

[1] Energhx Research Group, Department of Mechanical Engineering,
353 Faculty of Engineering, University of Lagos, Akoka-Yaba, Lagos 101017, Nigeria;
E-Mail: olumide.babarinsa@energhx.com

[2] Faculty of Engineering and Applied Science, University of Ontario Institute of Technology,
2000 Simcoe Street North, Oshawa, ON L1H 7K4, Canada; E-Mail: marc.rosen@uoit.ca

* Author to whom correspondence should be addressed; E-Mail: ogedengbe@energhx.com;
Tel.: +234-703-668-9827.

Abstract: Numerical simulation of a suspended stirrer within a homogenizing system is performed towards determining the mixing performance of a homogenizer. A two-dimensional finite volume formulation is developed for the cylindrical system that is used for the storage and stirring of biodegradable food waste from eatery centers. The numerical solver incorporates an analysis of the property distribution for viscous food waste in a storage tank, while coupling the impact of mixing on the slurry fluid. Partial differential equations, which describe the conservation of mass, momentum and energy, are applied. The simulation covers the mixing and heating cycles of the slurry. Using carrot-orange soup as the operating fluid (and its thermofluid properties) and assuming constant density and temperature-dependent viscosity, the velocity and temperature field distribution under the influence of the mixing source term are analyzed. A parametric assessment of the velocity and temperature fields is performed, and the results are expected to play a significant role in designing a homogenizer for biodegradable food waste.

Keywords: homogenizer; finite volume method; stirrer; food waste; biodigester

1. Introduction

Food waste is the second-largest category of municipal solid waste sent to landfills in the United States, accounting for approximately 18% of the waste stream [1]. Among other sources of biomass, this biodegradable material consists of food scraps from restaurants, produce markets, fish markets, school cafeterias, homes and wherever else food is prepared. Typical food waste is in solid form, containing 80%–90% moisture; this implies that treatment, such as incineration, cannot be applied [2]. However, dumping of food waste in landfills generates methane, a potent greenhouse gas. Consequently, many research efforts have been devoted to the treatment of food waste in order to explore the possibilities of energy recovery from such a feedstock and to prevent its adverse environmental effects.

Anaerobic digestion of biodegradable food waste is the most common approach and offers the most cost-effective treatment, due to its high energy recovery and low environmental impact [3]. For sludge stabilization, this process helps with the co-digestion of sewage, leading to benefits, like the dilution of potential toxic compounds, an improved balance of nutrients, synergistic effects regarding microorganisms, an increased load of biodegradable organic matter and improved yield [4]. In a study by the East Bay Municipal Utility District, Oakland, CA, USA [1], it was revealed that food waste has up to three times as much energy potential as bio-solids. As energy prices continue to rise and countries seek renewable energy generation and energy independence, exploiting the energy from food waste is expected to become increasingly important.

Effective pre-treatment of food waste is important for the performance of a biogas plant. This pre-treatment starts with the collection of the biodegradable food waste from eatery centers for sequential discharge into a homogenizer, by the use of a macerator pump (see Figure 1). In the homogenizer, the food waste is conditioned into a slurry and held for a maximum of two weeks before it is transferred into an anaerobic digester. Apart from the production of slurry, the agitating and stirring effects of the homogenizer prevent sedimentation of the food waste.
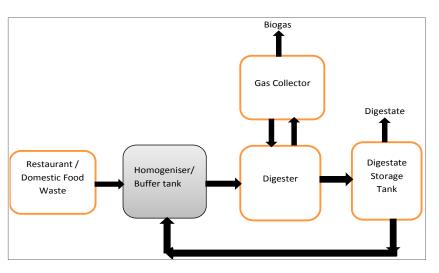
Figure 1. Process flow diagram for food waste digestion.

In a continuous processing system, digesters are equipped with a preparation tank where various substrates are mixed and prepared for loading [2]. The feedstock production, storage and supply are important parts of the bio-mass to bio-energy conversion chain [5]. In an organic waste biodegradability

test, Gibson *et al.* [6] homogenized a waste mixture (85% food waste) with a mechanical mixer for two and a half hours at 60 °C before it was subjected to pasteurization and thermal hydrolysis. Wang *et al.* [7] also exposed food waste meant for digestion to two types of thermal pre-treatment: 70 °C for two hours or 150 °C for one hour. An efficient storage or holding tank is required to ensure the food waste is properly pre-conditioned. Apart from the existence of other pre-conditioning treatments, the mixing process is significant to the performance of a homogenizer.

Various approaches have been applied to simulating the mixing of fluids in tanks and vessels. Harvey and Greaves [8] propose the impeller boundary condition approach, which depends on experimental data. Further improvements have been contributed by other investigators, including the use of the multiple rotating frame approach, which requires a longer time for convergence [9], and the sliding mesh approach, which uses large computational resources [10]. Irrespective of the size of computational resources demanded, the numerical treatment of the momentum source term approach [11], which incorporates the mixing or stirring effect in the momentum transports within the computational domain, represents the main portion of the tasks in the design of a homogenizer.

The aim of this article is to develop a mixing or stirring source model that couples with a two-dimensional finite volume formulation of the velocity and temperature distribution. A parametric analysis of the effects of different configurations of the stirrer is performed in order to provide insights for designers of homogenizers.

2. Finite Volume Formulation

2.1. Governing Equations of Viscous Food Waste

A mixture of food waste with low moisture content behaves like a slurry and appears to contain particles that, in most cases, are several orders of magnitude above the continuum length scale. Examples of other fluids within this category are clay suspended in water, toothpaste, blood, paper pulp suspended in water, oil-well drilling fluid, *etc.* [12]. Although a mixture with continuum size particles is actually a "two-phase flow" problem, there is no well-defined particle size above which mixtures cease to be considered uniform fluids. Especially when the material has a reasonably high moisture content, it can be treated as a uniform fluid with Newtonian characteristics. The selected mixture of food waste in this study fits this condition and, thus, is treated in this manner. Therefore, the basic equations that govern the mathematical modeling of flow processes are the mass, momentum and energy conservation equations.

The pumping process of the moisture-rich food waste through the combination of the macerator pump and a water dilute line enables the input of liquid food, assumed as a special incompressible, Newtonian fluid with temperature-dependent viscosity. Using a two-dimensional, transient Navier-Stokes equations with body force and a source term, we can write the following:

Continuity Equation:

$$\frac{\partial \rho}{\partial t} + \frac{\partial (\rho u)}{\partial x} + \frac{\partial (\rho v)}{\partial y} = 0 \tag{1}$$

Momentum Equations:

$$\rho \left(\frac{\partial u}{\partial t} + u \frac{\partial u}{\partial x} + v \frac{\partial u}{\partial y} \right) = -\frac{\partial p}{\partial x} + \frac{\partial}{\partial x}\left(\mu \frac{\partial u}{\partial x} \right) + \frac{\partial}{\partial y}\left(\mu \frac{\partial u}{\partial y} \right) + F \tag{2}$$

$$\rho \left(\frac{\partial v}{\partial t} + u \frac{\partial v}{\partial x} + v \frac{\partial v}{\partial y} \right) = -\frac{\partial p}{\partial y} + \frac{\partial}{\partial x}\left(\mu \frac{\partial v}{\partial x} \right) + \frac{\partial}{\partial y}\left(\mu \frac{\partial v}{\partial y} \right) + \rho g + F \tag{3}$$

Energy Equation:

$$\frac{\partial T}{\partial t} + u \frac{\partial T}{\partial x} + v \frac{\partial T}{\partial y} = \frac{k}{\rho c}\left[\frac{\partial}{\partial x}\left(\frac{\partial T}{\partial x} \right) + \frac{\partial}{\partial y}\left(\frac{\partial T}{\partial y} \right) \right] \tag{4}$$

where t denotes time, k the thermal conductivity of the fluid, g the acceleration due to gravity, ρ the density of the fluid and c the specific heat capacity of the fluid. Furthermore, u and v denote the fluid velocity components.

The source term F in Equations (2) and (3) is derived from the force impact of the impeller on the fluid. This force is equal to the product of the mass flow rate across the interaction section and the fluid velocity variation around the blade [13]. The substantial fluid velocity variation around the blade is equal to the resultant velocity from the interaction of the fluid and the impeller blade. Mathematically, we can write:

$$F = \rho V^2 A \tag{5}$$

where:

$$V^2 = (wr)^2 - u^2 \tag{6}$$

Here, w denotes the rotational speed for the impeller (in rad/s), r the radius of the impeller and A the blade surface area. This analogy assumes that the frictional force due to the impeller action on the fluid is negligible.

2.2. Formulation with Dirichlet Boundary Conditions

Equations (1) to (6) are formulated using a two-dimensional finite volume computation domain. Figure 2 shows the control volumes for a typical staggered grid discretization of the domain. Using the Semi-Implicit Method for Pressure-Linked Equations Consistent (SIMPLEC) algorithm [14,15], Ogedengbe *et al.* [16] proposed Non-Inverted Skew Upwind Scheme (NISUS)-based multiple upstream nodes for convective interpolation. Since the detailed implementation of this formulation is covered elsewhere [15], the imposition of the Dirichlet boundary conditions is focused on here. It is assumed that fluid velocity and temperature at all fluid-solid boundaries are equal to the corresponding values for the solid boundary. The boundary conditions used are $T = T_w = 333$ K, $u = 0$ and $v = 0$ at the top surface, bottom surface and side walls. The initial conditions used are $T = T_{ref} = 301$ K, $u = 0$ and $v = 0$. The model liquid is taken to have constant properties, except for its viscosity, which is taken to vary with temperature.

Considering the fact that the integration of Equations (1) to (4) over the control volumes typified by Figure 2 are represented by the standard summation form [15], we can write:

$$a_p \phi_p = \sum a_{nb} \phi_{nb} + b \tag{7}$$

where a, ϕ and b refer to the finite volume coefficient, the scalar variable (such as the nodal temperature in the energy equation) and the source term, respectively. The imposed Dirichlet boundary conditions across the walls of the homogenizer represent the isothermal assumption of the heat carrier from the concentrated solar energy via the micro-solar collector (see Figure 3).
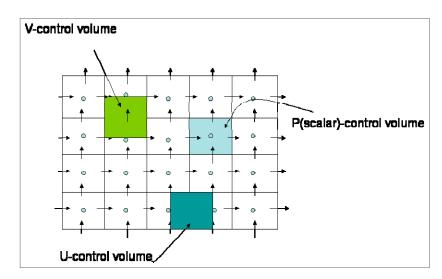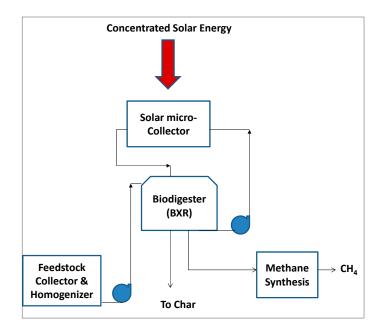
Figure 2. A typical staggered finite volume computational domain.

Figure 3. Configuration of a concentrating solar power (CSP)-driven biodigester system.

2.3. Numerical Simulation

The geometry of the simulated tank is shown in Figure 4. The homogenizer is modeled with a two-dimensional rectangular domain and a centered vertical-axis impeller. The diameter of the cylindrical vessel B is 0.30 m, while the height of the vessel H is 0.375 m. Numerical simulations are conducted at four rotational speeds of the impeller, *i.e.*, 50, 150, 250 and 350 rpm.

Ordinarily, food waste materials are non-Newtonian, and hence, the viscosity is a function of shear rate and temperature, typically with a flow behavior index less than one. However, during forced convection heating, the shear rate is small, and hence, the viscosity may be assumed to be a function of temperature only [17]. Because of the low shear rate of the liquid food used in the simulation, the viscosity can be assumed independent of shear rate, so that the fluid behaves as a Newtonian fluid. In the simulation presented here, it is assumed that the viscosity can be calculated as a function of temperature [16]:

$$\mu = a + bT + cT^2 \tag{8}$$

where coefficients *a*, *b* and *c* are reported to be 1.47 Pa s, -4.21×10^{-2} Pa s K^{-1} and 3.15×10^{-4} Pa s K^{-2}, respectively.
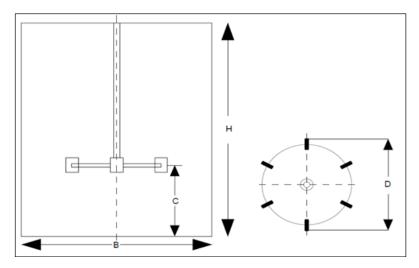
Figure 4. Sketch of the 2D model of the storage tank with impeller.

The properties of carrot-orange soup used in the simulation are listed in Table 1. An impeller of diameter 0.16 m is used in the simulation. Other properties of the impeller and tank are provided in Tables 1 and 2 [11].

Table 1. Thermophysical properties of the homogenizing system.

Fluid/Impeller Material	Density (kg/m³)	Specific Heat Capacity (J·kg⁻¹·K⁻¹)	Thermal Conductivity (W·m⁻¹·K⁻¹)
Carrot-orange soup	1026	3880	0.596
Stainless steel	8000	500	16.3

Table 2. Dimensions of the tank configuration.

Dimension	Value (m)
B	0.300
H	0.375
C	0.125
D	0.016

Notes: Tank configuration includes the following: the diameter of the tank (B); the height of the tank (H); the clearance of the impeller position from the bottom of tank (C); and the diameter of the blade axis (D).

3. Results and Discussion

Taking the diameter of the cylindrical vessel as $B = 0.30$ m and the height of the vessel as $H = 0.375$ m, the performances are simulated within a two-dimensional computational domain at rotational speeds of 100, 200, 300, 400 and 500 rpm using an impeller of radius 0.08 m. For each of the internal points, the velocity in the *x* and *y* directions are all set to zero, while the temperature is set to 303 K. All simulations are run on a 15×15 grid at a time step of 0.05 for 5000 time steps. For the boundary conditions, the top, bottom and sides are treated as no-slip. The temperature of the walls is fixed at 333 K.

Figures 5–10 show the predicted velocity field distribution. A minor difference can be seen in the two-dimensional flow velocities obtained for the different angular velocities. With an increase in the rotational speeds, the velocity of the fluid becomes high, and areas of high velocity increase. These trends are noticeable in the lower section of the domain. The fluid flows away from the wall, slightly directed towards the center, while it decreases sharply towards the corners of the wall. It can be clearly seen from these figures that with an increase in the rotational speed, the velocity becomes high and areas of high velocity increase. This is especially notable at the impeller section of the domain.
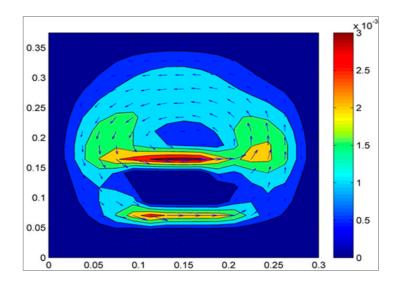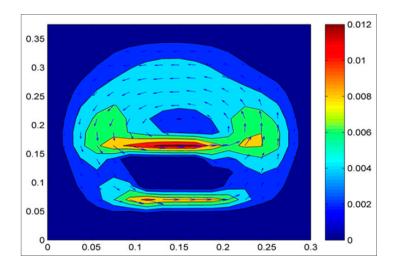
Figure 5. Two-dimensional flow velocity contour for an impeller speed of 50 rpm.

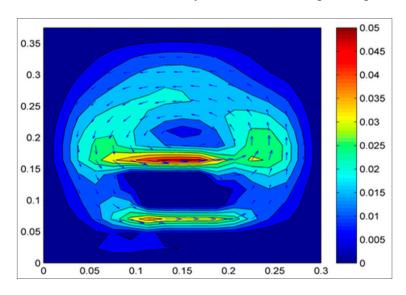**Figure 6.** Two-dimensional flow velocity contour for an impeller speed of 100 rpm.

Figure 7. Two-dimensional flow velocity contour for an impeller speed of 200 rpm.

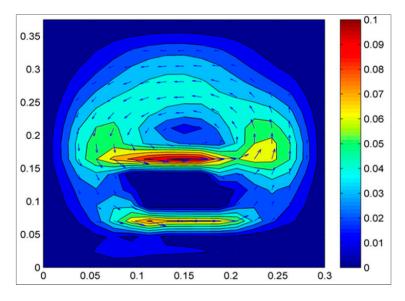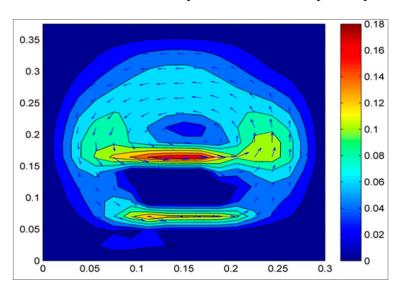**Figure 8.** Two-dimensional flow velocity contour for an impeller speed of 300 rpm.

Figure 9. Two-dimensional flow velocity contours for an impeller speed of 400 rpm.
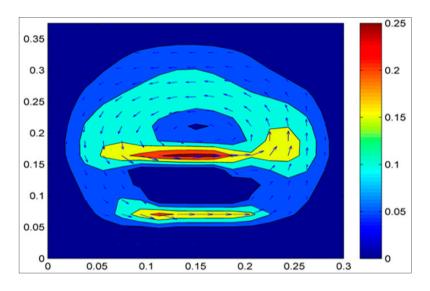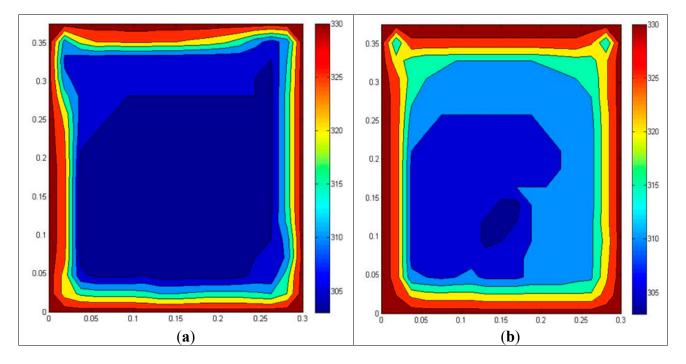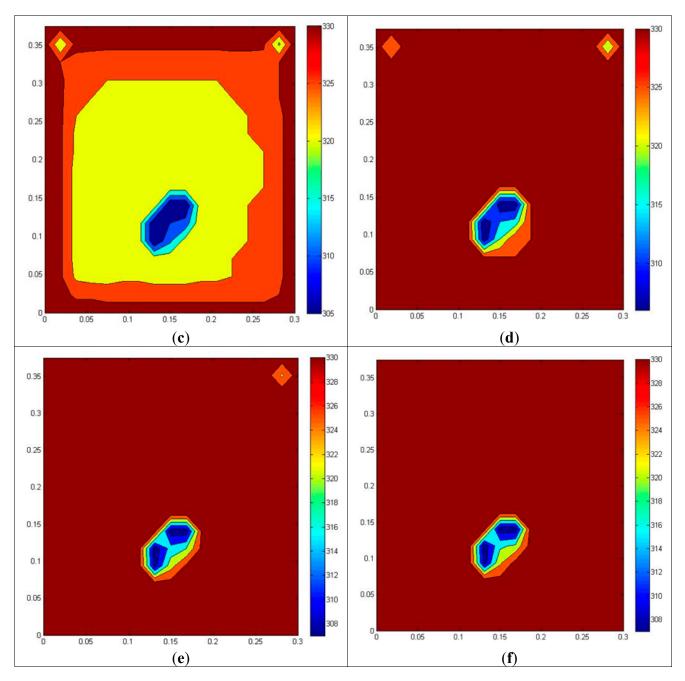
Figure 10. Two-dimensional flow velocity contour for an impeller speed of 500 rpm.

The temperature profile obtained in the homogenizer for all rotational speeds for the time considered is shown in Figure 11. The effect of the impeller in spreading the homogenizing temperature is observed to increase with the impeller speed. A large part of the fluid in the center is at 315 K. At a rotational speed of 200 rpm, the hotter temperature contours gradually move away from the wall of the homogenizer. The temperature patterns show that convective heat transfer generally dominates the entire fluid domain. The highest temperatures concentrate around the tank wall, while the lowest temperatures are found at the core of the tank. It can be clearly seen from these figures that with an increase in the rotational speed, the temperature becomes higher, and areas of high temperature increase until a constant temperature of 333 K is obtained throughout the domain.

Figure 11. Temperature distribution contours obtained in the homogenizer for various impeller rotational speeds: (**a**) 50 rpm; (**b**) 100 rpm; (**c**) 200 rpm; (**d**) 300 rpm; (**e**) 400 rpm; and (**f**) 500 rpm.

(**a**)

(**b**)

Figure 11. *Cont.*

(c)

(d)

(e)

(f)

4. Conclusions

The mixing performance of a stirrer in a homogenizing tank is investigated using a two-dimensional finite volume model of the mixer as a source term within the momentum transport. Using a temperature-dependent dynamic viscosity of moisture-rich carrot soup as an idealized Newtonian fluid, velocity and temperature contours are simulated at different rotational speeds of the impeller. It appears that the perfectly mixed region near the impeller expands with mixing and reduces the non-homogeneity in the tank. The results from the simulations show that increasing the impeller rotational speed improves both mixing effectiveness and heating. The application of the simulation results, with others, including the effects of different profiles and positioning of the impeller, could

lead to an improvement in the designs of homogenizers. This is an area of ongoing development for a concentrating solar power (CSP)-driven biodigester system.

Author Contributions

The paper represents contributions from the M.Sc. research of the first author (Olumide Babarinsa). The homogenizing system simulation study is part of the design and development of a CSP-driven biodigester project that is proposed and supervised by the second author (Emmanuel O.B. Ogedengbe) at the University of Lagos, Lagos, Nigeria. Extensive advice and critique of the research has been provided by the third author (Marc A. Rosen). All authors read and approved the final manuscript.

Conflicts of Interest

The authors declare no conflict of interest.

References

1. Gray, D.; Paul, S.; Cara, P. *Anaerobic Digestion of Food Waste, East Bay Municipal Utility District Report*; East Bay Municipal Utility: Oakland, CA, USA, 2008.
2. Zupančič, G.D.; Viktor, G. Anaerobic treatment and biogas production from organic waste. In *Management of Organic Waste*; Kumar, D.S., Bharti, A., Eds.; InTech: Rijeka, Croatia, 2012; pp. 1–28.
3. Mata-Alvarez, J.; Macé, S.; Llabrés, P. Anaerobic digestion of organic solid wastes: An overview of research achievements and perspectives. *Bioresour. Technol.* **2000**, *1*, 3–16.
4. Kubaska, M.; Sedlacek, S.; Bodik, I.; Kissova, B. *Food Waste as Biodegradable Substrates for Biogas Production Report*; Institute of Chemical and Environmental Engineering, Slovak University of Technology: Bratislava, Slovak Republic, 2010.
5. Ogedengbe, E.O.B.; Rosen, M.A. Electro-Kinetic pumping with slip irreversibility in heat exchange of CSP-powered bio-digester assemblies. *Entropy* **2012**, *12*, 2439–2455.
6. Gibson, T.; Smyth, M. *Organic Waste Biodegradability Test Bio Methane Potential Method Report*; Aqua Enviro: Wakefield, UK, 2007.
7. Wang, J.Y.; Liu, X.Y.; Kao, J.C.; Stabnikova, O. Digestion of pre-treated food waste in a Hybrid Anaerobic Solid–liquid (HASL) system. *J. Chem. Technol. Biotechnol.* **2006**, *3*, 345–351.
8. Harvey, P.S.; Greaves, M. Turbulent flow in an agitated vessel 2. Numerical-solution and model predictions. *Trans. Inst. Chem. Eng.* **1982**, *4*, 201–210.
9. Luo, J.Y.; Issa, R.I.; Gosman, A.D. Prediction of impeller-induced flows in mixing vessels using multiple frames of reference. In Proceedings of the 8th Europe Conference of Mixing, Cambridge, UK, 21–23 September 1994; pp. 155–162.
10. Mostek, M.; Kukukova, A.; Jahoda, M. Comparision of different techniques of modelling of flow field and homogenisation in stirred vessels. *Chem. Pap.* **2005**, *6*, 380–385.
11. Pericleous, K.A.; Patel, M.K. The modelling of tangential and axial agitators in chemical reactors. *Phys.Chim. Chem. Hydrodyn.* **1987**, *8*, 105–123.
12. Panton, R.L. *Incompressible Flow*, 2nd ed.; John Wiley & Sons: New York, NY, USA, 1996.

13. Huang, W.; Li, K. CFD simulation of flows in stirred tank reactors through prediction of momentum source. In *Nuclear Reactor Thermal Hydraulics and Other Applications*; Post Guillen, D., Ed.; InTech: Rijeka, Croatia, 2013; pp. 135–153.

14. Patankar, S.V. *Numerical Heat Transfer and Fluid Flow*; Hemisphere: Washington, DC, USA, 1980.

15. Van Doormaal, J.; Raithby, G.D. Enhancements of the SIMPLE for predicting incompressible fluid flows. *Numer. Heat Transf.* **1984**, *7*, 147–163.

16. Ogedengbe, E.O.B.; Naterer, G.F.; Rosen, M.A. Slip flow irreversibility of dissipative kinetic and internal energy exchange in microchannels. *J. Micromech. Microeng.* **2006**, *16*, 2167–2176.

17. Abdul Ghani, A.G. A Computer Simulation of heating and cooling liquid food during sterilization process using computational fluid dynamics. *Assoc. Comput. Mach. N. Z. Bull.* **2006**, *2*, 1–10.